Econ. Environ. Geol.
Vol. 32, No. 2, p. 129-139, 1999.

Hydrothermal Gold Mineralization of the Trabong District, Vietnam: Mineralogical and Geochemical Study

Jin-Kyun Han*, Chil-Sup So, Seong-Taek Yun**, Soon-Hak Kwon**, Kwang-Jun Choi**, Sang-Joon Pak** and Seon-Gyu Choi****

ABSTRACT : Hydrothermal gold deposits of the Trabong district in Vietnam occur as single-stage quartz ± calcite veins (0.3~1.2 m thick) which fill fault fractures in graphite-bearing gneiss and schist of the Chulai Complex and Kham Duc Formation of the Proterozoic age. Ore grades are 1.3 to 92.4 g/ton Au. Ore mineralogy is very simple, consisting mainly of pyrite with minor amounts of base-metal sulfides and electrum. Gold grains occur in two assemblages as follows: (1) early, Fe-rich (7.2~10.4 mole % FeS) sphalerite + electrum (50.4~64.3 atom % Au) assemblage occurring as inclusions in pyrite; (2) late, Fe-poor (<4.7 mole % FeS) sphalerite + galena + electrum (47.6~81.7 atom % Au) assemblage occurring along fractures of pyrites. Based on fluid inclusion data and thermochemical considerations of ore mineral assemblages, ore minerals were formed at high temperatures (about 230° to 420°C) from H_2O-CO_2(-CH_4)-NaCl fluids with the sulfur fugacity of about 10^{-6} to 10^{-10} atm. Fluid inclusion data also indicate that ore mineralization occurred mainly as a result of fluid unmixing accompanying CO_2 effervescence. Calculated oxygen and measured hydrogen isotope compositions of mineralizing waters ($\delta^{18}O_{V\text{-}SMOW}$ values = 5.3 to 8.6‰, $\delta D_{V\text{-}SMOW}$ values = −60 to −52‰), along with the sulfur isotope compositions of vein sulfides ($\delta^{34}S_{CDT}$ values = −1.2 to 2.8‰) and carbon isotope compositions of inclusion CO_2 ($\delta^{13}C_{PDB}$ values = −4.7 to −2.0‰) indicate that the high temperature (mesohypothermal) gold mineralization formed from a magmatic fluid.

Introduction

Hydrothermal fissure-filling gold deposits in the Trabong district (Fig. 1), located in central part (15° 13' to 15°20' N in latitude, 108° 15' to 108° 30' E in longitude) of the Vietnam, form one of the most important precious metal producers in the Vietnam. They were first discovered in 1936, and have been exploited intermittently until now. General ore grades are about 5. 2 to 92.4 g/ton Au and 0.2 to 63.5 g/ton Ag (KORES, 1997), indicating the relatively gold-rich nature of orebodies. Several areas in the district have been in active exploration. These include: Tranu and Tragiang areas with ore grades of trace to 92.4 g/ton Au without economic quantitites of silver; and Trakot and Trathuy areas with ore grades of 1.3 to 22.8 g/ton Au and 0.2 to 63.5 g/ton Ag (Fig. 1).

Previous studies on the Trabong district were performed mostly on stratigraphy, petrology, geological structures and mineralogical characteristics. Therefore, the genetic conditions and origin of gold mineralization have not been understood. The aims of this study are to document the nature of mineralization and to elucidate the origin and physicochemical conditions of auriferous fluids, based on mineralogical, fluid inclusion, and stable isotope data. This study will be helpful to guide the future exploration in the district.

* Korea Resources Cooperation, Seoul 156-010, Korea
** Department of Earth & Env. Sci., Korea University, Seoul 136-701, Korea, E-mail: styun@kuccnx.korea.ac.kr

General Geology and Ore Veins

Geology of the Trabong district consists of Proterozoic metamorphic rocks, Paleozoic metasedimentary and granitic rocks, and Cenozoic igneous rocks (Fig. 1). Detailed descriptions of geology are described in KORES (1997). The distribution of rock units seems to be largely controlled by an E-W-trending syncline developed in the central part of the district. Therefore, the younger rock units occur preferentially at central parts (Fig. 1).

The Proterozoic metamorphic rocks consist of the Kham Duc Formation and Chulai Complex. The Kham Duc Formation consists mainly of schist and is divided into three units (lower, middle, and upper units). The lower unit is found mainly in the southern-central part of the Trabong district, and is unconformable with the Chulai Complex. The unit is composed mineralogically of quartz, feldspars, biotite, muscovite, garnet and graphite. The middle unit are scattered preferentially in the northern part of the district, and consists of quartz, tremolite, biotite, pyroxene, feld-

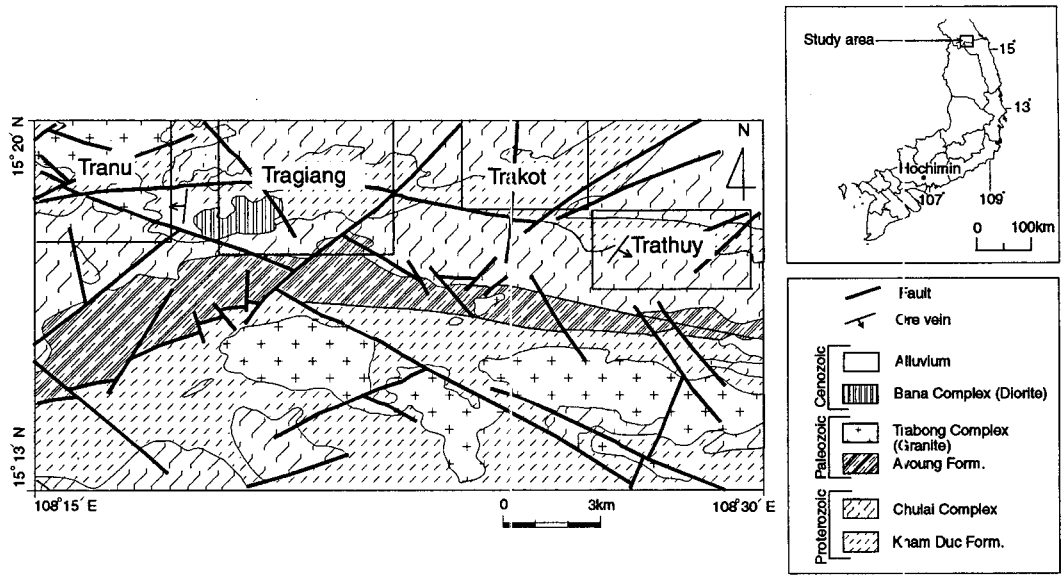

Fig. 1. Geologic map of the Trabong district, Vietnam (after KORES, 1997).

spars, hornblende and graphite. The upper unit is cropped out sparsely and is composed of quartz, K-feldspar, plagioclase, hornblende, biotite and pyroxene. The Chulai Complex consists of migmatitic gneiss and granitic gneiss. Migmatitic gneiss is widely distributed in the mineralized area, and is composed of quartz, plagioclase, microcline, biotite, sericite, chlorite and garnet. Granitic gneiss is also widespread in the district and is composed of K-feldspar, quartz, plagioclase, biotite, muscovite, sericite, and small amounts of chlorite and actinolite.

The Paleozoic granite (Trabong Granite or Complex) intrudes the Proterozoic metamorphic rocks and occurs as ubiquitous stocks (Fig. 1). It consists mainly of quartz, feldspars, biotite and hornblende. Along with Proterozoic metamorphic rocks, this granite hosts the gold-bearing veins. The Cenozoic Bana Complex occurs largely as diorite intruding Proterozoic metamorphic rocks.

Gold deposits in the Trabong district occur mostly as hydrothermal quartz veins that fill the open spaces along the faults and/or foliations in Proterozoic metamorphic rocks and Paleozoic granite. However, a few potential sites of gold mineralization also occur as disseminations in hydrothermally altered metamorphic rocks. In this study, we exclude the disseminated ores.

Quartz veins in the Trabong district are usually massive in appearance, but are locally vuggy at vein centers. The veins (several centimeters to 1.2 m wide) are highly variable in strike and dip directions, and can be traced at least by 10 to 300 m along the strike direction. Locally, dark graphite-rich bands with thickness of several centimeters are spatially associated with mineralized veins, and are thought to act as a reducing agent during the mineralization. Due to the pervasive surface weathering, the outcrops of veins typically show deep reddish color.

The Tranu-Tragiang area occupies the northwestern part of the Tragbong district, and comprises the Kham Duc Formation (mainly graphite schist), Chulai Complex (granitic gneiss and migmatitic gneiss), Trabong Granite, and Cenozoic Bana Complex (mainly diorite). Outcrops of quartz veins are 0.3 to 1.2 m wide and 50 to 300 m long. The veins are composed mainly of quartz with minor amounts of sulfides (mainly pyrite). Sulfides in veins are generally poor (usually <10 vol %) in amounts, but are locally enriched up to 70%.

The Trakot-Trathuy area occupies the northeastern part of the Trabong district, and comprises the Kham Duc Formation and Chulai Complex. Mineralized quartz veins (0.5 to 0.7 m thick) are often parallel to the foliation of Proterozoic metamorphic rocks, and generally strike N30-60°E with dips of 20~40° south or north. Pyrite is only recognizable in vein outcrops.

Mineral paragenesis and Thermochemical Conditions of Ore Deposition

The mineral paragenesis in veins of the Trabong district was constructed by examining the textures and mineral assemblages (Fig. 2). Chemical compositions

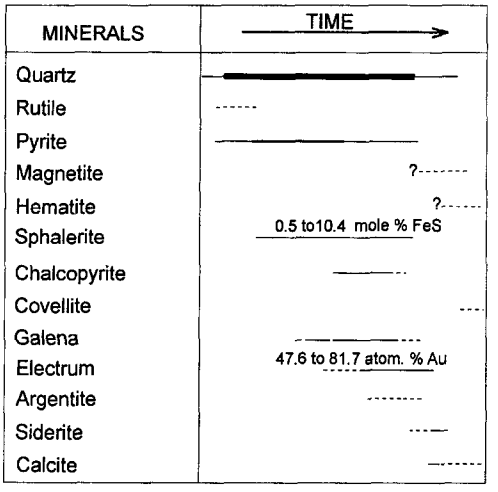

Fig. 2. Generalized paragenetic sequence of minerals from hydrothermal veins of the Trabong district.

Table 1. Chemical compositions of electrum and sphalerite from the Trabong distric, Vietnam.

Are	Type*	Electrum	Sphalerite
Tranu	I	–	7.2~8.3(N=7)
	II	47.6~68.4(N=13)	0.5~4.7(N=25)
Trathuy	I	50.4~64.3(N=6)	10.0~10.4(N=3)
	II	–	3.4~4.0(N=15)
Trakot	I	–	1.4~3.1(N=11)
	II	65.0~81.7(N=3)	–
Tragiang	I	–	–
	II	65.0~66.4(N=6)	–

* type I = occurring as inclusions in pyrite; type II = occurring as fracture fillings in pyrite.

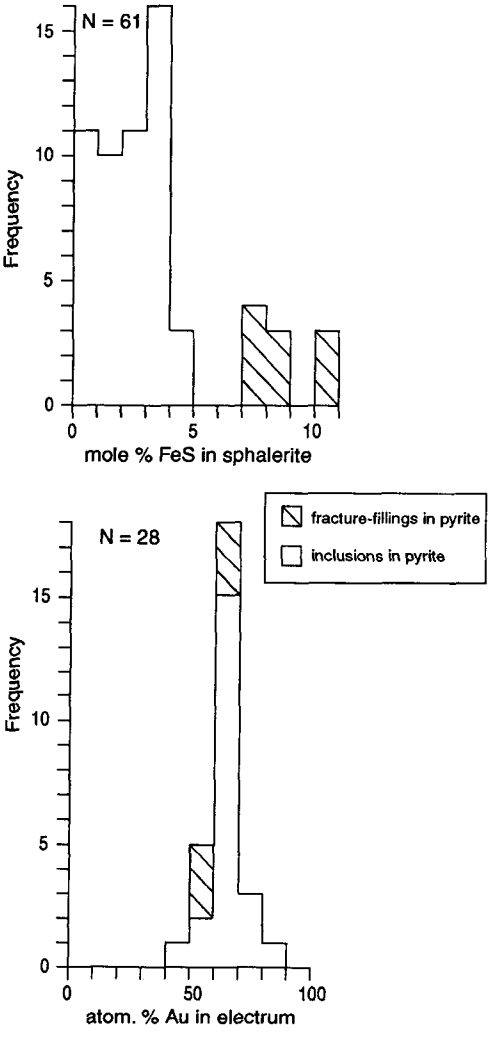

Fig. 3. Histograms showing chemical compositions of sphalerite and electrum from the Trabong district.

of sphalerite and electrum were also measured by the electron probe microanalyzer (JEOL Superprobe 8600SX at the Center for Mineral Resources Research), in order to examine the general compositional variations (Table 1, Fig. 3).

Ore mineralogy of veins in the Trabong district is very simple, consisting mainly of quartz with pyrite, sphalerite, galena, and rare amounts of chalcopyrite, electrum, magnetite, hematite and covellite, and is similar in different ore deposits. Hematite and covellite appear to be supergene alteration products.

Pyrite, the most abundant sulfide, occurs mainly as subhedral to euhedral grains (1 to 10 mm in size) which are disseminated throughout the veins. It is intergrown with sphalerite and galena. Some pyrites are fractured and infilled by gangues and ore minerals such as sphalerite, chalcopyrite, galena and electrum.

Sphalerite occurs as two types, based on time and assemblage: (1) early, small inclusions within pyrite, whose iron contents (number of analysis = 10) are 7.2 to 10.4 mole %; (2) late, anhedral grains occurring within fractures of pyrite, whose iron contents (N = 51) range from 0.5 to 4.7 mole %. The second type typically contains tiny inclusions of chalcopyrite. Chemical compositions of sphalerite do not show any spatial variation with different localities. Galena occurs along grain boundaries or fractures of pyrite or sphalerite, and is intergrown with late sphalerite and electrum.

Based on the occurrence, electrums can be classified into two types: (1) early, tiny inclusions (<5 μm in size) within pyrite, whose gold contents (N = 6) are 50.4 to 64.3 atom %; (2) late, anhedral grains (up to 50 μm in size) associated with sphalerite and galena along

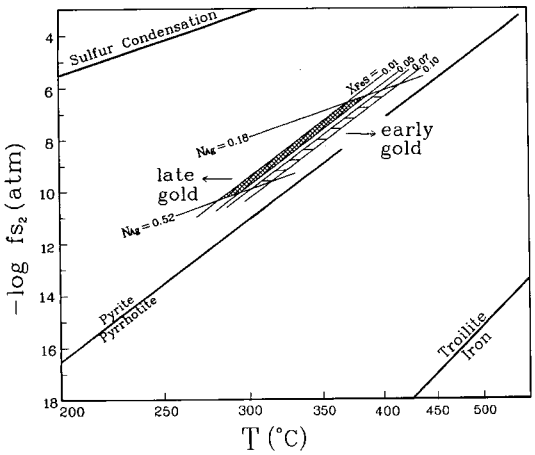

Fig. 4. Fugacity of sulfur versus temperature diagram showing depositional conditions of gold in the Trabong district.

fractures of pyrites, whose gold contents (N = 22) are 47.6 to 81.7 atom %.

Assuming that hydrothermal fluids and mineral assemblages were in chemical equilibrium, thermodynamic considerations were attempted to estimate the physicochemical conditions of hydrothermal fluids. A temperature versus sulfur fugacity (fs_2) diagram (Fig. 4) was constructed using the observed mineral assemblages and compositional data in the systems Fe-Zn-S (Barton, Toulmin, 1966; Barton, Skinner, 1979) and Au-Ag-S (Barton, Toulmin, 1964).

The early assemblage consisting of pyrite + Fe-rich sphalerite (7.2 to 10.4 mole % FeS) + electrum (50.4 to 64.3 atom % Au) was formed from the fluid with log fs_2 and temperature values of -6.2 to -9.7 atm and 310° to 420°C, respectively. On the other hand, the late assemblage consisting of Fe-poor sphalerite (0.5 to 4.7 mole % FeS) + galena + late pyrite + chalcopyrite + electrum (47.6 to 81.7 atom. % Au), occurring along fractures of pyrite and quartz, was precipitated from the fluid with log fs_2 and temperature conditions of -6.5 to -10.3 atm and 270° to 370°C (Fig. 4). This calculation suggests that gold precipitation in the Trabong district occurred mainly as a result of temperature decrease, possibly associated with the unmixing of fluids (see below).

Fluid Inclusion Study

Thirty vein quartz samples were collected from underground ore stopes and outcrops, and were examined for microthermometric measurements in order to determine the temporal and spatial variations of temperature and composition of auriferous hydrothermal fluids. Sphalerite was not suitable for study because of the opacity. Microthermometric data were obtained on a FLUID Inc. gas-flow heating/freezing stage which was calibrated with synthetic CO_2 and H_2O inclusions. Temperatures of total homogenization (Th-total) have the standard error of ±2°C, whereas temperatures of carbonaceous phase homogenization (Th-CO_2) and of melting of carbonaceous phase (Tm-CO_2), ice (Tm-ice), and CO_2-clathrate (Tm-clathrate) have standard errors of ±0.2°C. Salinity data were obtained based on freezing-point depression in the system H_2O-NaCl for aqueous inclusions (Bodnar, 1993) and on clathrate melting temperatures for liquid CO_2-bearing inclusions (Collins, 1979; Diamond, 1992).

Occurrence and compositional types of fluid inclusions

Vein quartz samples examined are usually inclusion-rich, probably due to repeated fracturing and healing during and after the quartz deposition. The size of fluid inclusions ranges widely from <3 to 30 μm. Two main types of fluid inclusions were identified on the basis of the phase relations recognized at room temperatures or during freezing runs (Table 2): type I (liquid-rich, aqueous) and type II (liquid CO_2-bearing).

Type I inclusions consist of two phases (H_2O-rich, liquid and vapor) at room temperature. The gas bubble comprises 5 to 45% of the total inclusion volume. They occur either in isolated, regular-shaped inclusions or in trails along healed fractures, indicating their both primary and secondary origin (Roedder, 1984). Some primary inclusions recognizably form clathrates during freezing runs, indicating the presence of minor amounts of CO_2 (about 0.85 molal; Hedenquist, Henley, 1985). Type I inclusions homogenize to the liquid phase upon heating.

Type II inclusions contain three phases (liquid CO_2, vapor CO_2, and a H_2O-rich liquid) at or near room temperatures, and occur only as primary inclusions. They occupy more than about half of the numbers of primary inclusions in all samples examined. Type II inclusions can be further classified into two subtypes, based on the relative abundance of carbonaceous phase and the homogenization mode: type IIa ($H_2O \geq CO_2$ in volume %, homogenizing to an aqueous liquid) and type IIb ($CO_2 > H_2O$, homogenizing to a carbonaceous vapor). Volumetric proportions of CO_2 (liquid + vapor) at room temperature are usually about 10 to 50% for type IIa inclusions and about 60 to 90% for type IIb inclusions. Type II inclusions usually decrepitate upon heating due to the build-up of high internal pressures. These two subtype inclusions occur together and show the whole range of

Table 2. Summary of microthermometric data of fluid inclusions in vein quartz from gold deposits in Trabong district.

Area	Inclusion type[1)]	Occurrence[2)]	Tm-CO_2 (°C)	Th-CO_2 (°C)	Tm-clathrate (°C)	Tm-ice (°C)	Th-total (°C)	Estimated salinity (wt. % NaCl)
Tranu and	I	P	–	–	–	−1.2~−9.2	232~357	2.1~13.1
Tragiang		S	–	–	–	−0.4~−0.9	157~238	0.7~1.6
	IIa	P	−56.6~−59.4	20.4~29.4	6.0~11.2	–	261~343	1.6~7.4
	IIb	P	−56.8~−61.8	15.6~28.5	6.2~8.6	–	263~337	2.8~7.1
Trakot and	I	P	–	–	–	−0.4~−8.9	253~411	0.7~12.7
Trathuy		S	–	–	–	−0.5~−7.6	181~254	0.9~11.1
	IIa	P	−56.6~−65.6	17.3~29.8	5.9~11.6	–	240~344	0.6~7.6
	IIb	P	−56.7~−58.7	11.5~28.7	6.1~9.7	–	253~399	0.6~7.3

[1)] I=aqueous, liquid-rich; IIa=liquid CO_2-bearing ($H_2O \geq CO_2$); IIb=liquid CO_2-bearing ($CO_2 > H_2O$)
[2)] Based on normal criteria of Roedder (1984). P=primary; S=obvious secondary.

CO_2 volume within individual samples, indicating the history of pervasive fluid unmixing accompanying CO_2 effervescence.

Microthermometric data

Microthermometric data of fluid inclusions are shown in Table 2 and Fig. 5 to 10.

The melting and homogenization of CO_2 in type II inclusions occurred at temperatures of −56.6° to −65.6°C and of 11.5° to 29.8°c (all to the liquid), respectively (Figs. 5 and 6). The low Tm-CO_2 values (down to −65.6°C, especially for the Trakot and Trathuy area; Fig. 5) suggest the presence of CH_4 in addition to CO_2 in carbonaceous phase, as the CH_4 component which is miscible with CO_2 lowers Tm-CO_2 considerably (Burruss, 1981; Heyen *et al.*, 1982). However, for most type II inclusions the closeness of the Tm-CO_2 data to those of pure CO_2 (−56.6°C; see Fig. 5) indicates that the amounts of CH_4 in most of type II inclusions are relatively low. The Th-CO_2 values were variable within single samples, possibly suggesting that the density of carbonaceous phase was highly variable during the time of entrapment. Assuming that the carbonaceous phase is composed predo- minantly of CO_2 without CH_4, the measured Th-CO_2 data imply the density of CO_2 ranging from about 0.60 to 0.85 g/cm^3 (Bodnar *et al.*, 1985).

The Tm-clathrate values of type II inclusions range from 5.9° to 11.6°C (Fig. 7). Except for some inclusions with the values of higher than 10.0°C (corresponding to the Tm-clathrate value of pure CO_2 clathrate; Bozzo *et al.*, 1975), the measured Tm-clathrate values correspond to the salinities of less than 7.6 wt. % eq. NaCl if we assume that type II inclusions belong to the H_2O-CO_2-NaCl system without CH_4 (Diamond, 1992). Some Tm-clathrate data of >10.0°C

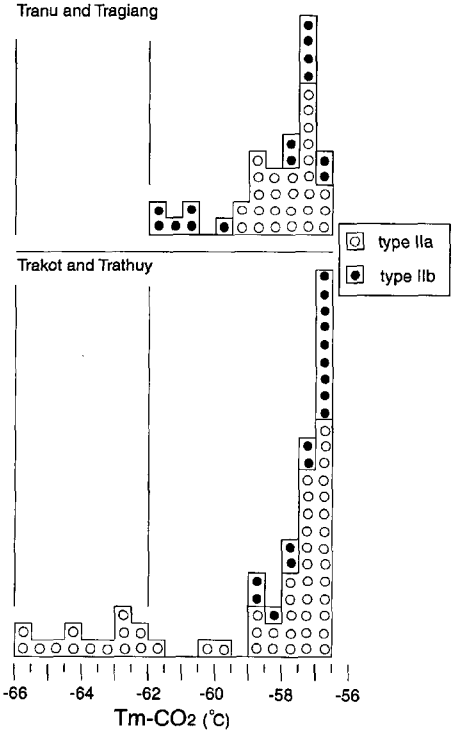

Fig. 5. Melting temperatures of CO_2 (Tm-CO_2) in carbonaceous (type II) fluid inclusions in vein quartz.

are thought to indicate the presence of CH_4 in carbonaceous phase because the formation of CH_4 clathrate will raise the clathrate melting temperature (Hollister, Burruss, 1976; Burruss, 1981). Although many type II inclusions decrepitated prior to the total homogenization, we could obtain some numbers of Th-total data through slow heating. The Th-total data obtained range from 240° to 344°C (Fig. 8).

Primary type I (aqueous) inclusions have the Tm-ice

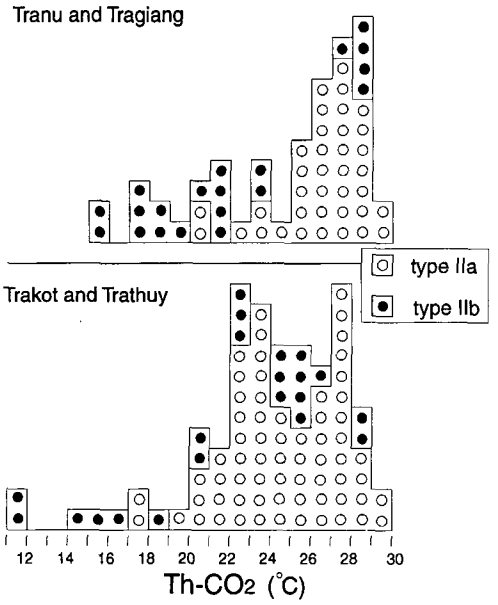

Fig. 6. Homogenization temperatures of CO_2 ($Th\text{-}CO_2$) in carbonaceous (type II) fluid inclusions in vein quartz.

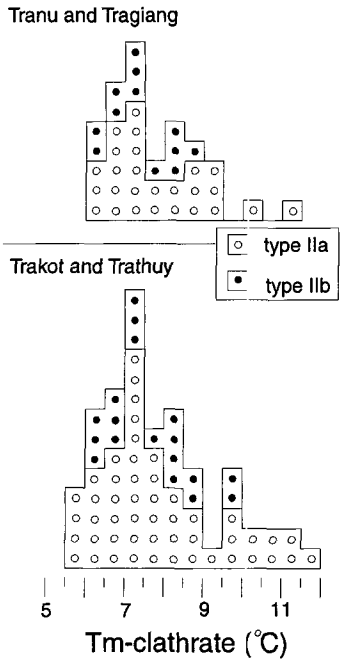

Fig. 7. Homogenization temperatures of CO_2-clathrate (Tm-clathrate) in carbonaceous (type II) fluid inclusions in vein quartz.

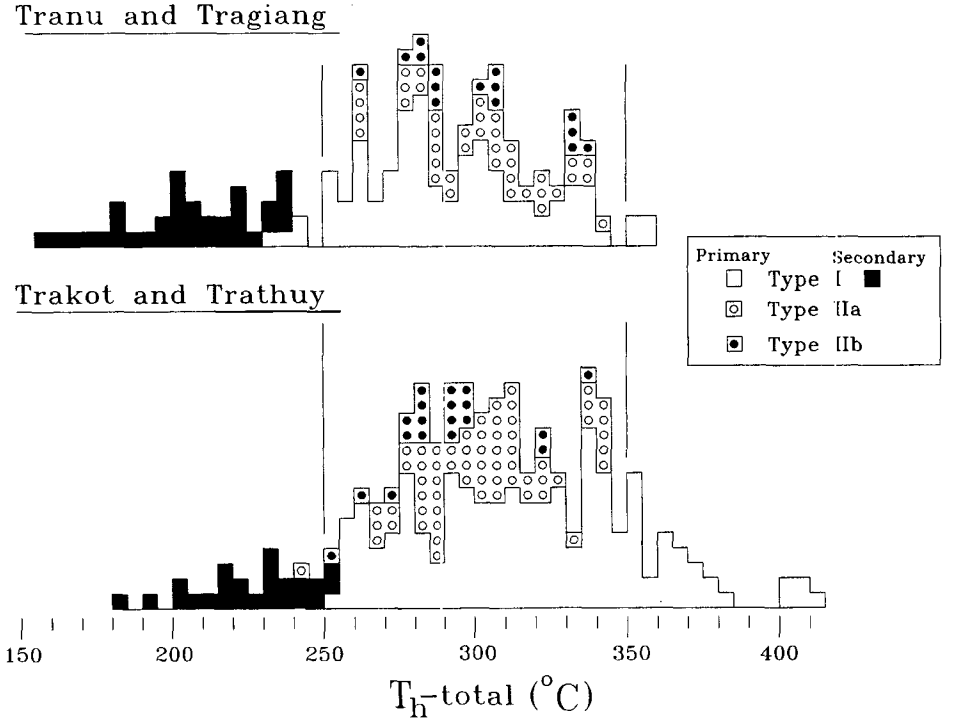

Fig. 8. Total homogenization temperatures (Th-total) of fluid inclusions in vein quartz.

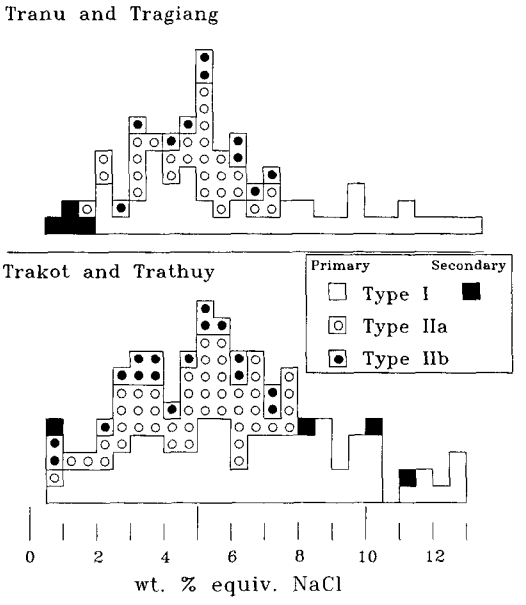

Fig. 9. Salinities of fluid inclusions in vein quartz.

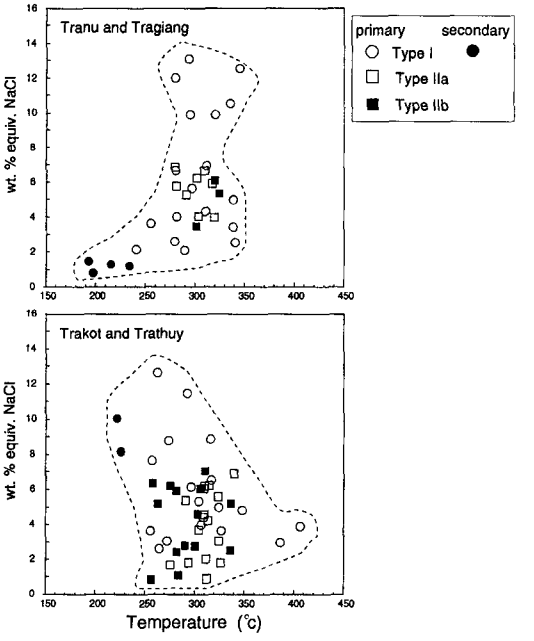

Fig. 10. Total homogenization temperature versus salinity diagram for fluid inclusions in vein quartz.

values of $-0.4°$ to $-9.2°C$, corresponding to the salinities of 0.7 to 13.1 wt. % eq. NaCl (if neglect the clathrate formation by which the ice melting points can be depressed to some dregrees; Hedenquist, Henley, 1985). They homogenize totally to the liquid phase at temperatures between 232° to 411°C (Figs. 8 and 9). Obvious secondary fluid inclusions are all type I with homogenization temperatures and salinities of 157° to 254°C and 0.7 to 11.1 wt. % eq. NaCl, respectively (Figs. 8 and 9).

The Th-total data of primary fluid inclusions in vein quartz range widely from about 230° to 410°C, and indicate that the deposition of quartz was most active at temperatures around 280~350°C (Fig. 8). The Th-total data agree well with the calculated temperatures based on the thermodynamic consideration of ore mineral assemblage (270~420°C). The wide range of homogenization temperatures possibly resulted from long and repeated history of fracturing and rehealing of veins (cf. So, Yun, 1997). The coexisting, primary type I (aqueous) and type II (carbonaceous) inclusions homogenize at temperatures between about 240° and 340°C. We consider that active CO_2 unmixing occurred at these temperatures.

Temporal evolution of ore fluids, and gold deposition

Fluid inclusion data characterized by both high homogenization temperatures (up to about 410°C) and common occurrence of liquid CO_2-bearing inclusions indicate the mesothermal to hypothermal conditions of gold deposition in the Trabong district, as is also indicated by the massive appearance and simple mineralogy of ore veins. The observed Tm-CO_2 and Th-CO_2 covariations for some type II inclusions indicate the presence of minor amounts of CH_4 (less than about 20 mole %, but mostly < 5 mole %) in CO_2 phase (Heyen *et al.*, 1982). Therefore, type II fluid inclusions are thought to belong to the H_2O-CO_2-NaCl system with minor amounts of CH_4.

The relationships between Th-total data and salinity for fluid inclusions in vein quartz are shown in Fig. 10. There is a trend of increasing salinity with decreasing temperature for primary fluid inclusions (especially for fluid inclusions from the Trakot-Trathuy area), although the trend is not so distinct with scattering of salinity. This relationship can be explained by the heterogeneity of hydrothermal fluids, probably related to the fluid unmixing accompanying CO_2 effervescence. Both the coexistence of type I (aqueous) and type II (carbonaceous) inclusions and the variability of CO_2 phase volume for type II inclusions also evidence that the fluid unmixing accompanying CO_2 effervescence was a major control of the evolution of auriferous fluids.

Fluid unmixing in hydrothermal systems would effectively result in abrupt physicochemical changes of hydrothermal fluids (e.g., decreases in temperature and molalities of ΣCO_2 and ΣH_2S, and increase in pH).

Gold is generally transported as $Au(HS)_2^-$ in relatively chloride-poor mesohypothermal fluids. Deposition of gold through destabilization of $Au(HS)_2^-$ may be represented by the reaction $Au(HS)_2^- + 1/2H_2(g) + H^+ \rightarrow Au + 2H_2S(aq)$, and results either from the decrease of $m_{\Sigma H2S}$ (so-called the desulfidation; Neall, Phillips, 1987) and temperature or from the increase of pH (e. g., Walsh *et al.*, 1988; Lu, Seccombe, 1993; Groves, Foster, 1993). Given the frequent association of sulfide minerals (pyrite, sphalerite, galena) with gold grains in the Trabong district, the role of sulfide precipitation accompanying the decreases of $m_{\Sigma H2S}$ and temperature is possibly critical. Therefore, the decreases of sulfur activity and temperature which accompany CO_2 effervescence, through sulfide deposition and/or H_2S loss, is likely the most important mechanism for gold deposition in high-temperature hydrothermal veins of the Trabong district.

The present results of fluid inclusion study (see Fig. 8) tend to show the more abundance of carbonaceous type II inclusions (relative to aqueous type I inclusions) in vein quartz from the Trakot-Trathy area (eastern part in the Trabong district) than the Tranu-Tragiang area (western part). If considered that the dominance of type II inclusions reflects the more intensive CO_2 effervescence of hydrothermal fluids, we may suggest that the Trakot-Trathy area seems to be more promising target of economic gold mineralization than other areas. Furthermore, the following features may be used to estimate the mineralization potential in the district: (1) more intensive hydrothermal alteration with larger amounts of disseminated pyrites and other sulfide minerals, which may reflect the larger degrees of desulfidation reaction, (2) the occurrence of veins with larger amounts of sulfide minerals (mainly pyrites) and carbonate minerals, and (3) the more frequent occurrence of type II fluid inclusions in vein quartz.

Table 3. Sulfur isotope data of sulfide minerals from mesothermal Au deposits in the Trabong district.

Area	Sample No.	Mineral	$\delta^{34}S$ (‰)	T(°C)[1]	$\delta^{34}S_{H2S}$ (‰)[2]
Tranu	V3-A1-1	Pyrite	1.5	280	1.4
	V3-A1-1	sphalerite	−0.1	280	−0.4
	V3-A2-1	pyrite	2.8	330	1.7
	V3-A2-2	galena	−1.2	290	−1.0
	V3-A4-1	pyrite	2.0	330	0.9
	V3-A4-2	galena	−0.1	300	1.8
Tragiang	V7-D-1	pyrite	2.3	350	1.3
Trakot	N1-D-1	pyrite	−0.1	300	−1.3
Trathuy	T6-A-1	pyrite	1.7	310	0.5
	T6-A-2	sphalerite	0.6	280	0.3

[1] Based on homogenization temperatures of fluid inclusions
[2] Calculated based on isotope fractionation equations in Ohmoto, Rye (1979).

Light Stable Isotope Study

In this study, we measured sulfur isotope compositions of sulfides, oxygen isotope compositions of quartz, and hydrogen and carbon isotope compositions of inclusion fluids extracted by crushing of quartz. Standard techniques for extraction and analysis were used, as described by McCrea (1950), Grinenko (1962), and Hall, Friedman (1963). Isotopic data are reported in standard notation relative to the CDT standard for sulfur, the PDB standard for C, and the V-SMOW standard for oxygen and hydrogen. The standard error of each analysis is about ±0.1‰ for C, O and S, and ±2‰ for H (Tables 3 and 4).

Sulfur isotope

Sulfur isotope analysis was performed on 10 hand-picked sulfide minerals. Sulfide minerals have the

Table 4. Oxygen, carbon, and hydrogen isotope data of quartz and their inclusion fluids from mesothermal Au deposits in the Trabong district.

Area	Sample No.	Mineral	$\delta^{18}O$(‰)	$\delta^{13}C_{CO2}$(‰)[1]	T(°C)[2]	$\delta^{18}O_{water}$(‰)[3]	δD_{water}(‰)
Tranu	V3-A-2	quartz	13.2		320	7.0	−60
Trakot	N1-B-1	quartz	12.2	−3.1	300	5.3	−52
	N1-C-1	quartz	13.9	−4.7	350	8.5	−56
	N1-C-2	quartz	13.4		340	7.3	−58
	N1-D-2	quartz	13.5		330	7.5	−59
Trathuy	T6-B-1	quartz	14.2	−2.0	330	8.3	−56
	T6-B-2	quartz	14.3		330	8.4	−55

[1] Carbon isotope compositions of CO_2 in inclusion fluids
[2] Based on fluid inclusion homogenization temperatures (average value of each sample) and paragenetic constraints
[3] Calculated based on quartz-water oxygen isotope fractionation equation in Matsuhisa *et al.* (1979).

following $\delta^{34}S$ values (Table 3): pyrite, −0.1 to 2.8‰; sphalerite, −0.1 to 0.6‰; galena, −0.1 to −1.2‰.

Assuming appropriate depositional temperatures (based on the temperature estimates by fluid inclusions and thermochemical studies: see Table 3), the $\delta^{34}S$ values of H_2S in hydrothermal fluids were calculated using the fractionation equations in Ohmoto, Rye (1979). The calculated $\delta^{34}S_{H2S}$ values range from −1.3 to 1.8‰ and do not show any temporal and spatial change (Table 3). Assuming that the estimated $\delta^{34}S_{H2S}$ values represent the sulfur isotope composition of the entire fluid ($\delta^{34}S_{\Sigma S}$), as is indicated by both the pyrite-dominant sulfide mineralogy and the sericite- and quartz-rich alteration mineralogy (Ohmoto, Rye, 1979), we consider that the sulfur isotope data likely indicate an igneous source of sulfur.

Carbon, oxygen, and hydrogen isotopes

The $\delta^{13}C$, $\delta^{18}O$ and D values for vein quartz and extracted inclusion fluids are summarized in Table 4.

Inclusion waters from vein quartz have the $\delta^{13}C_{CO2}$ values of −4.7 to −2.0‰. Seven samples of vein quartz were measured for oxygen isotope compositions, and have the $\delta^{18}O_{V\text{-}SMOW}$ values ranging narrowly from 12.2 to 14.3‰. Using the quartz-water oxygen isotope fractionation equation of Matsuhisa *et al.* (1979), coupled with average homogenization temperatures of fluid inclusions in each sample, the calculated $\delta^{18}O_{V\text{-}SMOW}$ values of waters range from 5.3 to 8.6‰. Seven inclusion waters were extracted from quartz samples which were selected to contain large proportions of primary fluid inclusions. They have very uniform $\delta D_{V\text{-}SMOW}$ values falling between −52 and −60‰ (Table 4).

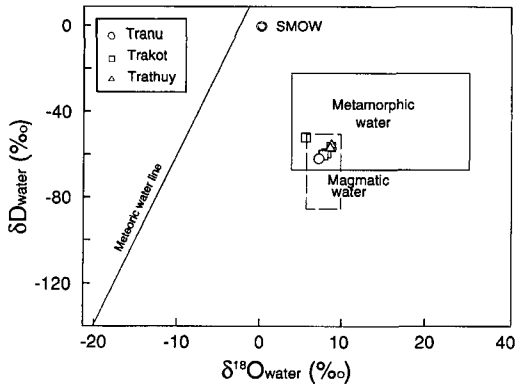

Fig. 11. Hydrogen versus oxygen isotope diagram showing isotope compositions of hydrothermal fluids formed in the Trabong district. The general magmatic and metamorphic water boxes are from Taylor (1979). Note that the fluid's $\delta^{18}O$-δD estimates fall in the magmatic water box.

The measured and calculated, oxygen and hydrogen isotope compositions of the hydrothermal fluids can be used to assess the importance of meteoric, magmatic, and metamorphic waters in the auriferous hydrothermal system (Fig. 11). Our data fall within the primary magmatic water box (Taylor, 1979). Therefore, we consider that the mesothermal to hypothermal mineralization in the Trabong district formed from a magmatic fluid, possibly from nearby granitic rocks.

Summary

1. Gold vein deposits of the Trabong district in Vietnam are found in the Trakot, Trathuy, Tranu, and Tragiang areas. These deposits consist of mineralogically simple quartz ± calcite veins infilling the fault fractures in Proterozoic, graphite-bearing gneiss and schist of the Chulai Complex and Kham Duc Forma- tion. The veins are gold-rich with ore grades of 1.3 to 92.4 g/ton Au.

2. Vein mineralogy consists dominantly of pyrite with minor amounts of base-metal sulfides such as sphalerite, galena and chalcopyrite. Gold occurs as electrums associated with sulfide minerals, and form two distinct assemblages: (1) early assemblage occurring as inclusions in pyrite and consisting of Fe-rich sphalerite (7.2~10.4 mole % FeS) and electrum (50.4~64.3 atom % Au); (2) late assemblage occurring within fractures of pyrite and consisting of Fe-poor sphalerite (<4.7 mole % FeS), galena and electrum (47.6~81.7 atom % Au). Thermochemical considerations of ore mineral assemblages indicate that gold deposition occurred from high-temperature (270~420°C) fluids with the sulfur fugacity of about 10^{-6} to 10^{-10} atm.

3. Fluid inclusions in vein quartz consist of two types: liquid CO_2-bearing, and aqueous liquid-rich. Liquid CO_2-bearing inclusions characteristically occur in the district, and are highly variable in CO_2 content. Low melting temperatures of frozen CO_2 (down to −65.6°C) indicate the presence of CH_4 (<5 to 20 mole %) in carbonaceous phase. Ore mineralization formed at high temperatures (230~420°C) from H_2O-CO_2(-CH_4)-NaCl fluids, and occurred mainly through fluid unmixing accompanying CO_2 effervescence. Within the Trabong district, the Trakot-Trathuy area (eastern part) seems to be more promising target of economic gold mineralization than other areas.

4. Calculated oxygen and measured hydrogen isotope compositions of hydrothermal waters ($\delta^{18}O_{V\text{-}SMOW}$ values = 5.3 to 8.6‰, $\delta D_{V\text{-}SMOW}$ values = −60 to −52‰), along with the sulfur isotope compositions of vein sulfides ($\delta^{34}S_{CDT}$ values = −1.2 to 2.8‰) and carbon

isotope compositions of inclusion CO_2 ($\delta^{13}C_{PDB}$ values = −4.7 to −2.0‰) indicate that mesohypothermal gold mineralization formed from a magmatic fluid.

Acknowledgements

This study was supported by the Center for Mineral Resources Research (CMR), Korea University. The Special Research Fund of Korea University (given to C.S. So) was also helpful for this study. We thank Mr. K.Y. Shim for his help on fluid inclusion study. Constructive comments by Prof. I.S. Lee and Dr. I.J. Kim improved the manuscript.

References

Barton, P.B.Jr. and Skinner, B.J. (1979) Sulfide mineral stabilities, in Barnes, H.L., ed., Geochemistry of hydrothermal ore deposits. New York, Wiley Intersci., p. 278-403.

Barton, P.B.Jr. and Toulmin, P.III (1964) The electrum tarnish method for the determination of the fugacity of sulfur in laboratory sulfide systems. Geochim. Cosmochim. Acta, v. 28, p. 619-640.

Barton, P.B.Jr. and Toulmin, P.III (1966) Phase relations involving sphalerite in the Fe-Zn-S system. Econ Geol., v. 61, p. 815-849.

Bodnar, R.J. (1993) Revised equation and table for determining the freezing point depression of H_2O-NaCl solutions. Geochim. Cosmochim. Acta, v. 57, p. 683-684.

Bodnar, R.J., Reynolds, T.J. and Kuehn, C.A. (1985) Fluid inclusion systematics in epithermal systems. Rev. Econ. Geol., Volume 2, p. 73-97.

Bozzo, A.T., Chen, H.S., Kass, J.R. and Barduhn, A.J. (1975) The properties of hydrates of chlorine and carbon dioxide. Desalination, v. 16, p. 1209-1221.

Burruss, R.C. (1981) Analysis of phase equilibria in C-O-H-S fluid inclusions. Mineralog. Assoc. Canada Short Course Handb., v. 6, p. 39-74.

Collins, P.L.F. (1979) Gas hydrates in CO_2-bearing fluid inclusions and the use of freezing data for estimation of salinity. Econ. Geol., v. 74, p. 1435-1444.

Diamond, L.W. (1992) Stability of CO_2 clathrate hydrate + CO_2 liquid + CO_2 vapour + aqueous KCl-NaCl solutions: Experimental determination and application to salinity estimations of fluid inclusions. Geochim. Cosmochim. Acta, v. 56, p. 273-280.

Grinenko, V.H. (1962) Preparation of sulfur dioxide for isotopic analysis. Zeitschr. Neorganische. Khimii, v. 7, p. 2478-2483.

Groves, D.I. and Foster, R.P. (1993) Archaean lode gold deposits, in Foster, R.P., ed., Gold metallogeny and exploration. London, Chapman and Hall, p. 63-103.

Hall, W.E. and Friedman, I. (1963) Composition of fluid inclusions Cave-In-Rock fluorite district, Illinois and upper Mississippi Valley zinc-lead district. Econ. Geol., v. 56, p. 886-911

Hedenquist, J.W. and Henley, R.W. (1985) The impotance of CO_2 on freezing point measurements of fluid inclusions: Evidence from active geothermal systems and implications for epithermal ore deposition. Econ. Geol., v. 80, p. 1379-1406.

Heyen, G., Ramboz, C. and Dubessy, J. (1982) Modelling of phase equilibria in the CO_2-CH_4 below 50°C and 100 bar: Application to inclusion fluids. Acad. Sci. Paris Comptes Rendus, v. 294, p. 203-206.

Hollister, L.S. and Burruss, R.C. (1976) Phase equilibria in fluid inclusions from the Khtada Lake metamorphic complex. Geochim. Cosmochim. Acta, v. 40, p. 163-175.

KORES (Korea Resources Cooperation) (1997) Report on the joints geological and mineral survey in Trabong-Tramy area, Quang Ngai-Quang Nam province, the Socialist Republic of Vietnam. Phase I, 161p.

Lu, J. and Seccombe, P.K. (1993) Fluid evolution in a slate-belt gold deposit-a fluid inclusion study of the Hill End goldfield, NSW, Australia. Mineral. Deposita, v. 28, p. 310-323.

Matsuhisa, Y., Goldsmith, R. and Clayton, R.N. (1979) Oxygen isotope fractionation in the system quartz-albite-anorthite-water. Geochim Cosmochim. Acta, v. 43, p. 1131-1140.

McCrea, J.M. (1950) The isotopic chemistry of carbonate and a paleotemperature scale. Jour. Chem. Physics, v. 18, p. 849-857.

Neall, F.B. and Phillips, G.N. (1987) Fluid-wall rock interaction in an Archean hydrothermal gold deposit: A thermodynamic model for the Hunt mine, Kambalda. Econ. Geol., v. 82, p. 1679-1694.

Ohmoto, H. and Rye, R.O. (1979) Isotopes of sulfur and carbon, in Barnes, H.L., ed., Geochemistry of hydrothermal ore deposits. New York, Wiley Intersci., p. 509-567.

Roedder, E. (1984) Fluid inclusions. Rev. Mineralogy, v. 12, 644 p.

So, C.S. and Yun, S.T. (1997) Jurassic mesothermal gold mineralization of the Samhwanghak mine, Youngdong district, Republic of Korea: Constraints on hydrothermal fluid geochemistry. Econ. Geol., v. 92, p. 60-80.

Taylor, H.P.Jr. (1979) Oxygen and hydrogen isotope relationships in hydrothermal mineral deposits, in Barnes, H.L., eds., Geochemistry of hydrothermal ore deposits. New York, Wiley Intersci., p, 236-277.

Walsh, J.F., Kesler, S.E., Duff, D. and Cloke, P.L. (1988) Fluid inclusion geochemistry of high-grade, vein-hosted gold ore at the Pamour mine, Porcupine camp, Ontario. Econ. Geol, v. 83, p. 1347-1367.

1998년 10월 19일 원고접수, 1999년 2월 19일 게재승인.

베트남 짜봉(Trabong) 지역의 열수 금 광화작용: 광물 및 지화학적 연구

한진균 · 소칠섭 · 윤성택 · 권순학 · 최광준 · 박상준 · 최선규

요 약 : 베트남 짜봉 지역의 열수 금광상은 단일 광화 시기의 석영±방해석 맥(폭 0.3~1.2 m)으로 산출되며, 원생대의 Chulai Complex와 Kham Duc Formation을 이루는 함 흑연 편마암 및 편암 내의 단층 열극을 충진하고 있다. 광석의 금 품위는 1.3~92.4 g/ton이다. 광석 광물은 매우 단순하여 주로 황철석 및 미량의 base-metal 황화물과 에렉트럼으로 구성된다. 금은 다음과 같은 두 유형의 공생군에서 산출된다: (1) 함철량이 풍부한 섬아연석(7.2~10.4 mole % FeS)+엘렉트럼(50.4~64.3 atom % Au) 공생군으로서 황철석 내의 내포물로 산출되며 초기에 해당; (2) 함철량이 낮은 섬아연석(<4.7 mole % FeS)+방연석+엘렉트럼(47.6~81.7 atom % Au) 공생군으로서 황철석의 단열을 따라 산출되며 후기에 해당. 유체포유물 자료 및 공생 광물군에 대한 열역학적 고찰에 의하면, 광화작용은 H_2O-CO_2(-CH_4)-NaCl계 유체로부터 230~420℃의 고온에서 진행되었으며 광화 유체의 황 분압은 10^{-6}-10^{-10} atm이었다. 광석 광물의 침전은 주로 CO_2 개스의 일탈을 수반한 유체 불혼화에 의해 진행되었다. 광화 유체 중 물의 산소 및 수소 동위원소 조성($\delta^{18}O_{V\text{-}SMOW}$ 값 = 5.3 to 8.6‰, $\delta D_{V\text{-}SMOW}$ 값 = −60 to −52‰)과 황화 광물의 황 동위원소 조성($\delta^{34}S_{CDT}$ 값 = −1.2 to 2.8‰) 및 유체포유물 CO_2의 탄소 동위원소 조성($\delta^{13}C_{PDB}$ 값 = −4.7 to −2.0‰)은 본 연구 지역의 중-고온형 금 광화작용이 마그마성 유체로부터 진행되었음을 지시한다.